Journal of KSNVE, Vol. 7, No. 2, pp. 209~214, 1997.

(Original Paper)

Identification of Crack Orientation in a Simple Rotor

회전체에서의 균열 방위 결정

Oh Sung Jun, Chong-Won Lee and Byoung Duk Lim
전 오 성* · 이 종 원** · 임 병 덕***

(Received October 4, 1996 ; Accepted January 31, 1997)

Key Words : Rotor(회전체), Transverse Crack(횡균열), Orientation(방위), Harmonics(고조파), Simulation(시뮬레이션)

ABSTRACT

Vibration characteristics which are typical in a cracked rotor can be utilized for detection of crack. The changing trend of harmonics at the second harmonic resonant speed according to the crack depth and the unbalance orientation has been discussed. To characterize the vibration depending on crack orientation, the unbalance and gravitational responses of the cracked rotor are calculated. An algorithm for crack orientation identification is also introduced. A trial mass is attached step by step with even angle interval along a certain circumference, and then the synchronous and second horizontal harmonic components of vibration are measured and curve-fitted using least square method. Numerical simulations using this method show good results.

요 약

균열을 가진 회전축은 고조파성분이 진동에 나타나는 특징을 갖는다. 이 고조파성분을 균열탐지에 활용하기 위하여는 이들이 크게 발생되는 회전수를 이용할 필요가 있다. 2차고조파공진속도를 정의하여 이 속도에서의 균열과 불균형질량 방위각에 따른 고조파 진동 특성을 단순회전체에서 설명하였다. 이 특성을 이용하여 균열의 위치를 나타낼 수 있는 알고리즘을 만들고 수치실험을 하여 타당성을 보였다.

1. Introduction

Since the 1970s many works have been reported in the research area of cracked rotor modeling, dynamics analysis and diagnosis[1~8]. One of the ultimate objectives of the cracked rotor dynamics research is to derive the crack identification method.

Crack on shaft repeats opening and closing as the shaft rotates, and thus the transverse stiffness of shaft changes repeatedly. Since, however, the stiffness value forms not sinusoidal but periodic curve, the vibration response has harmonics. When one uses harmonics for crack detection, he may note that the harmonics have quite peculiar distribution pattern depending on the rotational speed. It is impor-

*Member, Dept. of Mechanical Engineering, Jeonju University, Jeonju, 560-759, Korea
**Member, Dept. of Mechanical Engineering, KAIST, Taejon, 305-701, Korea
***Member, School of Mechanical Engineering, Yeungnam University, Taegu, 712-749, Korea

tant for the use of harmonics to determine the proper rotational speed. In this study, considering that among the harmonics the second harmonic is likely to be the largest[7], the second harmonic resonant speed, where the second harmonic components of the vibration take the maximum amplitudes, is chosen.

Jun et. al[7] discussed the feature of the harmonics depending on the crack and unbalance directions. They showed that the synchronous and the second harmonics have their extreme values at pecular relative angles between the crack and the unbalance directions. The simulation results in reference[7] are introduced, in this study, to extract the feasible techniques for identification of crack direction calculating the unbalance and gravitational responses of the cracked rotor. The changing feature in peak -to-peak vibration depending on the unbalance orientation is used to derive a method of crack orientation identification.

2. Second Harmonic Resonant Speed

Unlike in the case of a rotor with no crack, the vibration of a cracked rotor due to the unbalance and gravity consists of many harmonics, and resonant speeds at which each harmonic component of response becomes maximum are no longer coincident with the nominal critical speeds or their integer fractions. Therefore it may be convenient to define the nth harmonic resonant speed as the rotational speed at which the nth harmonic component of

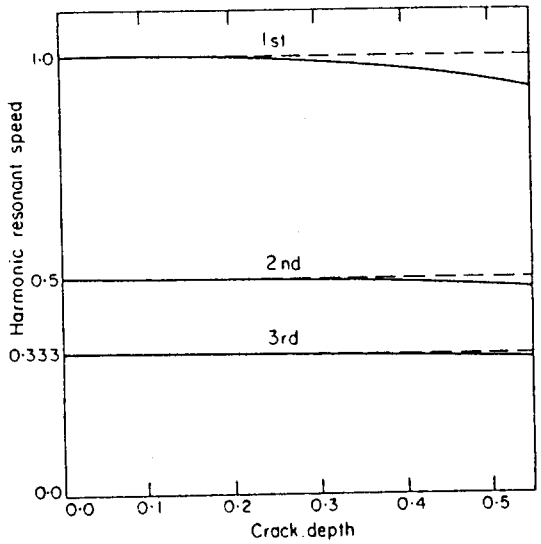

Fig. 1 Harmonic resonant speeds vs. crack depth (shaft length=700mm, diameter=15mm)

vibration takes the maximum amplitude. It should be noted that the vibration characteristics of a particular component are best seen near the corresponding harmonic resonant speed[7].

The typical harmonic resonant speeds monotonically decrease as the crack depth increases, as shown in Fig. 1. This is because the propagation of crack causes the decrease in shaft stiffness and thus the increase in vibration amplitude. In addition, the asymmetry in stiffness, due to the crack, causes the change in the response spectrum. Figure 2 shows the first and the second harmonic amplitudes of whirl vibration measured in the horizontal and the vertical axes at the second harmonic resonant speed. Dimensionless amplitude is the

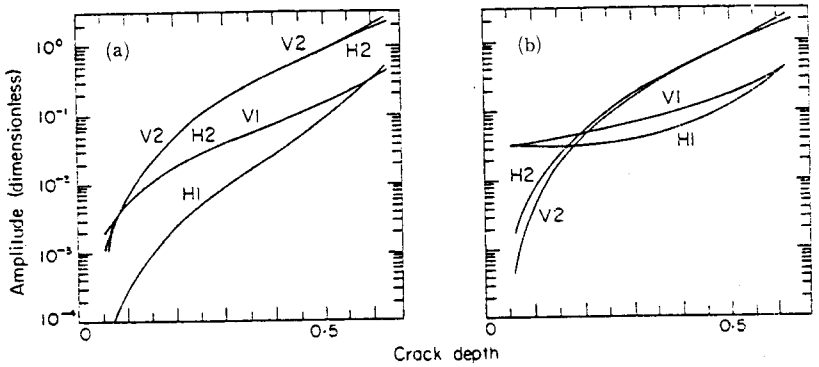

Fig. 2 Harmonic amplitudes at the second harmonic resonant speed with crack depth varied (damping ratio=0.02); (a) Without unbalance (b) Unbalance/static deflection=0.1 and unbalance on the crack direction.

amplitude divided by static deflection. H and V stand for the horizontal and the vertical components, respectively, and the numbers followed indicate the harmonic order. The results show that the vibration amplitudes increase rapidly with increasing crack depth. At the second harmonic resonant speed the third and higher harmonic amplitudes also increase with increasing crack depth, however, they are hardly measurable unless the crack develops to a considerable level. In particular, the second harmonics are very sensitive to the crack depth only, whereas the synchronous components are affected not only by the crack depth but by the unbalance, especially at small crack depth. Thus the second harmonics, magnified at the second harmonic resonant speed, can be used as good indicators for crack identification.

3. Identification Algorithm of Crack Orientation

3.1 Effect of unbalance orientation

Figure 3 shows the whirls observed at the second harmonic resonant speed when the crack depth and the orientation of unbalance with its magnitude unchanged vary. In figure, β is the unbalance orientation from crack. As mentioned previously, the increase of harmonics is notable with crack depth increased, and the whirl motion is sensitive to the unbalance orientation. Since the first (synchronous) and the second harmonic components tend to have maximum or minimum amplitudes when the unbalance is in-phase and out-of phase with respect to the crack[6], it is theoretically possible to detect the crack direction by shifting a trial unbalance along the periphery of the disk.

The extensive simulation studies were performed to check the practicality of the use of the second harmonic components to identify the crack. Figure 4 shows the directions of unbalance which induce the maximum and minimum amplitudes of the harmonic components. The unbalance direction is from the crack. The results show that the directions of the maximum and minimum values keep stable phase relative to the direction of unbalance.

3.2 Algorithm

The first and the second horizontal harmonics

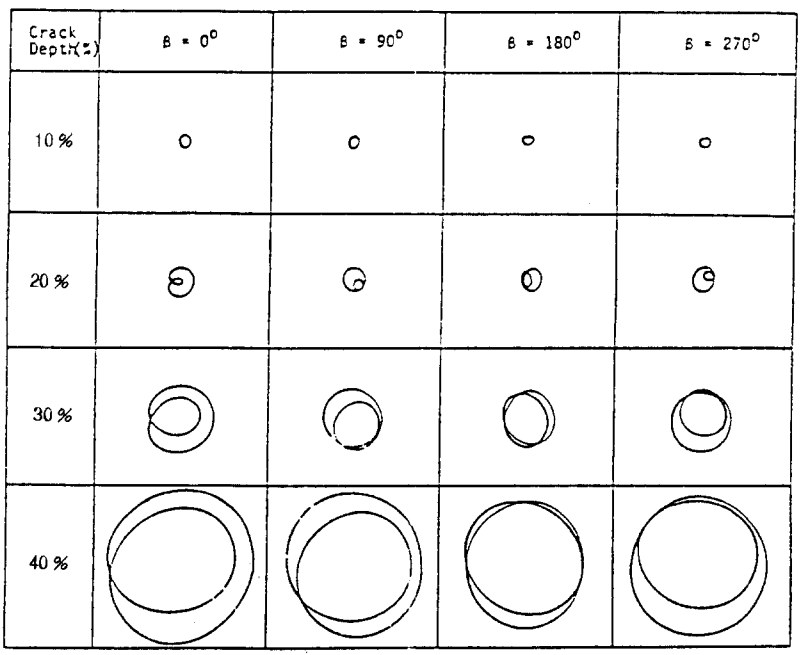

Fig. 3 Whirls at the second harmonic resonant speed with unbalance orientation changed (damping ratio=0.02 and unbalance/static deflection=0.1).

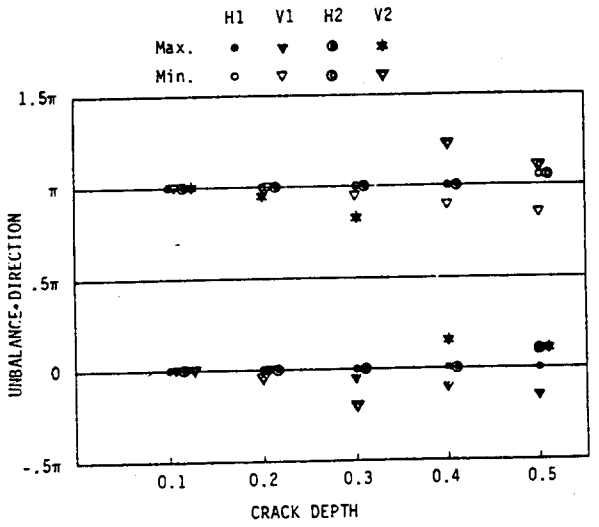

Fig. 4 Unbalance orientation inducing the maximum and minimum amplitudes of harmonics with the crack depth varied (damping ratio=0.02 and unbalance/static deflection=0.1).

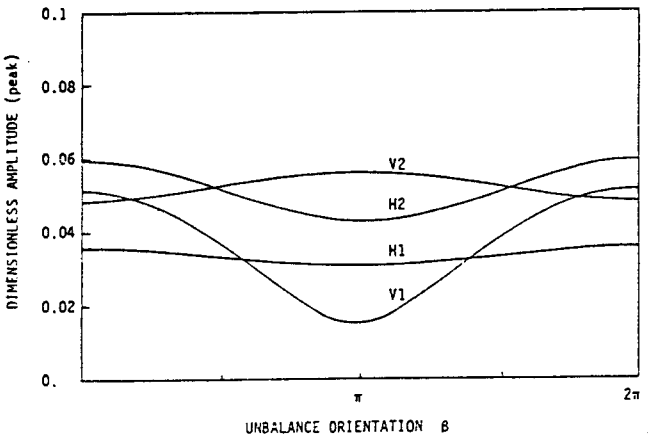

Fig. 5 Harmonics at the second harmonic resonant speed with crack orientation varied (damping ratio =0.02 and unbalance/static deflection = 0.1).

have their maximum and minimum values at the consistent positions of unbalance direction independently of crack depth, as shown in Fig. 4. The curves for $H1$ and $H2$ for typical case are shown in Fig. 5. These curves obtained from numerical simulation are very similar to cosine curve[7]. Here the curves for $H1$ and $H2$ are expressed as follows, for convenience,

$$X_1(\beta)=A_1\cos\beta+B_1 \tag{1}$$

$$X_2(\beta)=A_2\cos\beta+B_2 \tag{2}$$

Now a method for identifying the crack orientation is to be explained. Symbols used in deriving the algorithm are shown in Fig. 6. ξ_1 and η_1 are rotational coordinates, the origin of which is located at the center of shaft, and ε_t is the magnitude of trial mass to be attached in order to find the crack direction. ε_r and θ_r are the magnitude and the orientation of residual unbalance, θ_r is the direction of resultant centrifugal force due to the trial mass and the residual unbalance and α_c is the angle to be obtained here. This angle indicates where the crack exists from the position of the first trial mass attached.

If the value of X_1 is x_{1i} when the ith($i=1, 2,\cdots$, N : N the total number of trials) trial mass is

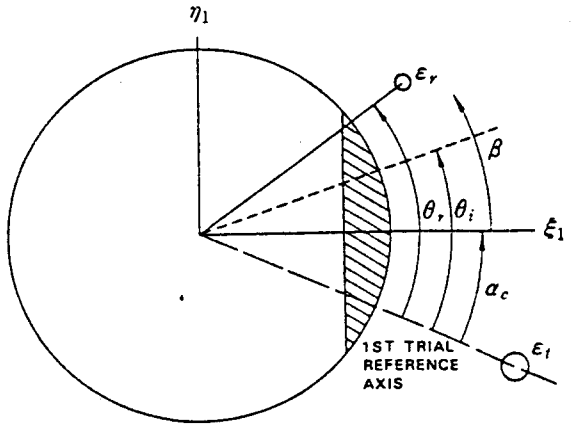

Fig. 6 Coordinates system for crack identification.

attached, from equation (1) the following equation is expressed:

$$x_{1i}=A_1\cos(\theta_i-\alpha_c)+B_1 \tag{3}$$

where

$$\theta_i=\tan^{-1}\frac{\varepsilon_r\sin\theta_r+\varepsilon_t\sin\dfrac{(i-1)2\pi}{N}}{\varepsilon_r\cos\theta_r+\varepsilon_t\cos\dfrac{(i-1)2\pi}{N}} \tag{4}$$

Introducing complex notation, the equation (3) becomes

$$x_{1i}=A_1Re[e^{j(\theta_i-\alpha_c)}]+B_1 \tag{5}$$

where $j=\sqrt{-1}$. Introducing an unit vector

$$e^{j\theta_i}=\frac{\varepsilon_re^{j\theta_r}+\varepsilon_te^{j\frac{(i-1)2\pi}{N}}}{|\varepsilon_re^{j\theta_r}+\varepsilon_te^{j\frac{(i-1)2\pi}{N}}|} \tag{6}$$

into equation (5) yields

$$x_{1i}=\frac{A_1 Re\left[\left(\varepsilon_r e^{j\theta_r}+\varepsilon_t e^{j\frac{(i-1)2\pi}{N}}\right)e^{-j\alpha_c}\right]}{\left|\varepsilon_r e^{j\theta_r}+\varepsilon_t e^{j\frac{(i-1)2\pi}{N}}\right|}+B_1 \quad (7)$$

Multiplying $\left|\varepsilon_r e^{j\theta_r}+\varepsilon_t e^{j\frac{(i-1)2\pi}{N}}\right|$ and summing $i=1$ to N yields

$$\sum_{i=1}^{N}(x_{1i}-B_1)\left|\varepsilon_r e^{j\theta_r}+\varepsilon_t e^{j\frac{(i-1)2\pi}{N}}\right|=NA_1 Re\left[\varepsilon_r e^{j(\theta_r-\alpha_c)}\right] \quad (8)$$

since

$$\sum_{i=1}^{N} e^{j\frac{(i-1)2\pi}{N}}=0 \quad (9)$$

If the residual unbalance is very small compared with the trial mass, the value inside absolute symbol of the left hand side of equation (8) can be expressed as ε_t approximately and that equation yields a simple form.

$$\mu_1\varepsilon_t=A_1 Re\left[\varepsilon_r e^{j(\theta_r-\alpha_c)}\right]+B_1\varepsilon_t \quad (10)$$

where

$$\mu_1=\frac{1}{N}\sum_{i=1}^{N}x_{1i} \quad (11)$$

When $\varepsilon_t \gg \varepsilon_r$, eliminating B_1 from equations (7) and (10) yields

$$\begin{aligned} x_{1i}&=A_1 Re\left[e^{j\frac{(i-1)2\pi}{N}}e^{-j\alpha_c}\right]+\mu_1 \\ &=A_1\cos\left((i-1)2\pi/N-\alpha_c\right)+\mu_1 \end{aligned} \quad (12)$$

This equation has almost the same form as equation (3), except that the residual unbalance term is cancelled explicitly and the unknown B_1 is replaced as the calculable value μ_1.

Using the same procedure, the equation (2) can also be expressed as

$$x_{2i}=A_2\cos\left((i-1)2\pi/N-\alpha_c\right)+\mu_2 \quad (13)$$

where

$$\mu_2=\frac{1}{N}\sum_{i=1}^{N}x_{2i} \quad (14)$$

If the trial mass is much larger than the residual unbalance, the equations (12) and (13) are usable in the identification of crack orientation. These equations have three unknowns A_1, A_2 and α_c. If the measured vibration amplitudes at the ith trial are x'_{1i} and x'_{2i}, the errors between these values and x_{1i} and x_{2i}, which have been assumed to exist on the exact cosine curves, are expressed as

$$\begin{aligned} Err_1=\sum_{i=1}^{N}&\left(A_1\cos\left((i-1)2\pi/N-\alpha_c\right)\right. \\ &\left.+\mu_1-x'_{1i}\right)^2 \end{aligned} \quad (15)$$

$$\begin{aligned} Err_2=\sum_{i=1}^{N}&\left(A_2\cos\left((i-1)2\pi/N-\alpha_c\right)\right. \\ &\left.+\mu_2-x'_{2i}\right)^2 \end{aligned} \quad (16)$$

Here μ_1 and μ_2 are replaced as follows

$$\mu_1=\frac{1}{N}\sum_{i=1}^{N}x'_{1i}, \quad \mu_2=\frac{1}{N}\sum_{i=1}^{N}x'_{2i}$$

The total error is obtained by binding the equations (15) and (16)

$$Error=Err_1+Err_2\cdot W \quad (17)$$

where W is an weighting constant introduced to reduce the additional error due to the relative magnitude of two error functions, *i. e.*,

$$W=\left(\frac{\max(x'_{1i})-\min(x'_{1i})}{\max(x'_{2i})-\min(x'_{2i})}\right)^2 \quad (18)$$

Then, the following conditions which minimize the equation (17) are obtained

$$\begin{aligned} &\frac{\partial Error}{\partial A_1}=0 \\ &\frac{\partial Error}{\partial A_2}=0 \\ &\frac{\partial Error}{\partial \alpha_c}=0 \end{aligned} \quad (19)$$

and by solving these nonlinear simultaneous equations numerically, the crack orientation α_c is obtained.

4. Numerical Simulation

Simulation results using the algorithm are shown in Table 1. The crack depth is 30% with respect to the shaft diameter. The total trial number N is fixed to 4. The trial mass is attached beginning from the first position along the same circumference by $\pi/2$ interval, to the spin direction. Instead of the experimental values x'_{1i} and x'_{2i}, the results simulated from the governing and the stiffness equations of this study are used. To solve the equations in (19), Newton-Raphson method is used. Table 1 shows the dependence of the final result upon the first trial mass position. At the first simulation, the first trial

Table 1 Dependence of final results on the first trial mass position.

No. simulation	true value α(radian)	estimated value $\hat{\alpha}$(radian)	Error $\lvert\alpha-\hat{\alpha}\rvert$
1	0	0.012	0.012
2	−0.314	−0.298	0.016
3	−0.628	−0.614	0.014
4	−0.942	−0.932	0.010
5	−1.257	−1.246	0.011
6	−1.571	−1.559	0.012

mass is attached on the crack direction. From the second simulation, the position of the first mass advances along the spin direction by $\pi/10$. Simulations show very small errors. The results also reveal that the synchronous and second harmonics (H 1 and H 2) curves of Fig. 5 are almost identical to exact cosine curves. The closer the curves H 1 and H 2 to exact cosine curves, the smaller the error of $\hat{\alpha}$.

5. Concluding Remarks

The changing trend of harmonics at the second harmonic resonant speed according to the crack depth and the unbalance orientation is used for crack identification.

The changing features, in peak-to-peak value, of the synchronous and the second harmonic vibrations depending on the unbalance orientation are implemented to derive the method of crack orientation identification. Based on the consistent features of the harmonics, two sinusoidal curves are assumed.

In the identification method, a trial mass is attached step by step with even angle interval along a certain circumference, and then the synchronous and second horizontal harmonic components of vibration are measured and curve fitted using the least square method. Examples of numerical simulation using this method show good results.

Acknowledgments

본 논문은 1995년도 전주대학교 학술연구조성비에 의해 연구되었음.

References

(1) Mayes, I. W. and Davies, W. G. R., 1976, The Vibrational Behavior of a Rotating Shaft System Containing a Transverse Crack, Institution of Mechanical Engineers Conference Publication, Vibration in Rotating Machinery, Paper No. C168/76.

(2) Dimarogonas, A. D. and Paipetis, S. A., 1983, Analytical Methods in Rotor Dynamics. London: Applied Science.

(3) Imam, I., Azzaro, S. H., Bankert, R. J. and Scheibel, J., 1989, Development of an On-Line Rotor Crack Detection and Monitoring System, J. of Vibration, Acoustics, Stress, and Reliability in Design, Trans. ASME, Vol. 111, pp. 241~250.

(4) Changhe, L., Bernasconi, O. and Xenophontidis, N., 1989, A Generalized Approach to the Dynamics of Cracked Shaft, J. of Vibration, Acoustics, Stress, and Reliability in Design, Trans. ASME, Vol. 111, pp. 257~263.

(5) Lee, C. -W., Yun, J. -S. and Jun, O. S., 1992, Modeling of a Simple Rotor with a Switching Crack and its Experimental Verification, J. of Vibration and Acoustics, Trans. ASME, Vol. 114, pp. 217~225.

(6) Ratan, S. and Rodriguez, J., 1992, Transient Dynamic Analysis of Rotors Using SMAC Techniques, J. of Vibration and Acoustics, Trans. ASME, Vol. 114, pp. 477~488.

(7) Jun, O. S., Eun, H. J., Earmme, Y. Y. and Lee, C. -W., 1992, Modelling and Vibration Analysis of a Simple Rotor with a Breathing Crack, J. of Sound and Vibration, Vol. 155, No. 2, pp. 273~290.

(8) Jun, O. S., Lee, C. -W., Earmme, Y. Y. and Eun, H. J., 1992, Analysis of Crack Growth in a Simple Rotor with a Breathing Crack, Machine Vibration, Vol. 1, pp. 231~235.